

Modelling a Partly Filled Road Tanker during an Emergency Braking

Frank Otremba, José A. Romero

Abstract—A testing procedure and simulation formulation are proposed to study the effect of sloshing cargoes on the braking efficiency of partly filled road tankers. The testing methodology involves the instrumentation of an articulated road tanker equipped with 8 chambers. As an average, these chambers are filled with water, at 65% of their capacity. The instrumentation includes speed and acceleration sensors as well as two pressure sensors mounted in two different chambers. A series of braking maneuvers were performed at different initial speeds. On the other hand, the simplified model to simulate the sloshing cargo – truck interaction during braking, involves a multibody scheme that includes both the vehicle and the cargo. Specifically, the sloshing cargo is simulated on the basis of the pendulum analogy. The pressure in the sensors, is calculated through the superposition of the horizontal and vertical hydrostatic effects. Results show good correlation with the experimental data.

Index Terms — Tank-trucks, sloshing, experimental approach, braking performance

I. INTRODUCTION

PARTLY filled tank trucks carrying sloshing cargoes are susceptible to show poor dynamic performance when carrying out steering or speed changing manoeuvres [1]. Such manoeuvres involve lateral or longitudinal accelerations exerted on the cargo-vehicle system that originate inertial forces that unbalance the distribution of tire loads. Such changes in the tire load distribution implies different safety and performance effects. From the safety perspective, a poor load distribution can reflect an imminent rollover crash, or affect the available friction force available for braking [2]. Sloshing effects can even affect the pavement damage potentials of such vehicles [3]. The braking mechanics of vehicles involves the dynamics of two torques acting on the wheel axle. On the one hand, the braking moment that the brake system exerts on the wheel axle, as a function of the brake system design and conditions. The second torque, on the other hand, derives from the tire – pavement interaction, which is called here the wheel rotating torque T_r . This turning torque keeps the wheel rotating, as a function of the available tire-pavement friction, and of the tire load. Figure 1 illustrates these two-torque arrangements.

Manuscript received May 02, 2017; revised May 08, 2017.
 Frank Otremba is with the Federal Institute for Materials Research and Testing (BAM), Unter den Eichen 44-46 12203, Berlin, Germany. (email: Frank.Otremba@bam.de) Tel.: +49 30 8104-1320.
 José A. Romero is with the Queretaro Autonomous University, Queretaro, Mexico (email:jaromero@uaq.mx).

While the magnitude of the braking torque T_b is a function of the braking system design and condition, the rotating torque's magnitude depends on the available braking force F_b and on the dimension of the tire R , according to the following expression:

$$T_r = F_b R \quad (1)$$

where R is the instantaneous distance (radius) between the tire-pavement contact point and the wheel rotation center;

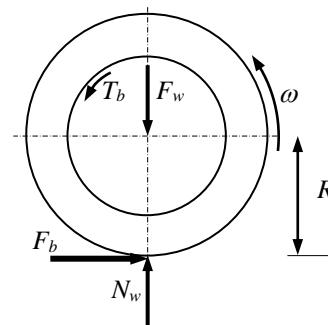


Fig. 1. Representation of the two torques acting on a vehicle's wheel.

and F_b depends on the braking coefficient and normal load N_w , as follows:

$$F_b = \mu N_w \quad (2)$$

The coefficient μ further depends on the slip angle between the tire and the pavement, as it is illustrated on Figure 2 for the case of a rubber tire on a dry asphalt pavement [4]. According with the data in Figure 2, the maximum braking coefficient will be in this case 0.75, for a slip angle of 0.2. Consequently, a low friction coefficient will occur when the wheel is completely locked. The aim of an antilock brake system is to maintain the wheel slip for a maximum braking coefficient. On the other hand, the normal force N_w in Eq. (2), will depend on the magnitude of the force at the tire-pavement interface. Such magnitude involves a static force

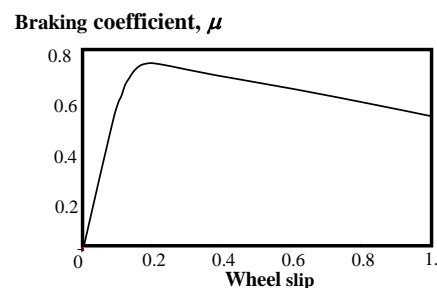


Fig. 2. Braking coefficient as a function of wheel-pavement slip.

to which a dynamic component is superimposed. While the static force depends on the distribution of the vehicle mass on its tires, the dynamic component of such a force will depend on the vibration behavior of the vehicle masses that integrate the vehicle, as a function of the perturbation exerted on them. This normal force directly affects the braking performance of a vehicle, so that the vehicle wheel can lock in case that the braking torque T_b is greater than the rotating torque T_r . Consequently, the braking performance of the vehicle will depend on the dynamic characteristics of the masses, springs and dampers that integrate the vehicle, as well as of the associated position of these components in the vehicle, and of the dimensions of the chassis.

In this context, when the vehicle carries a sloshing cargo, the vibration of such a mass will affect the overall vibration of the vehicle and, consequently, the magnitude of the normal forces N_w at the tire-pavement interface, further affecting the efficiency of the braking.

The behavior of vehicles carrying sloshing cargoes has been the subject of some research published in the literature. However, no research has reported the full-scale testing of a vehicle carrying a sloshing cargo when performing emergency braking maneuvers. In this paper, the results from a full-scale testing experiment are compared with a simplified simulation model involving a multibody and analogy approach. While the multibody approach considers the vehicle as integrated by solid rigid masses; the analogy model considers the sloshing cargo, as the response of an oscillating simple pendulum whose length is determined on the basis of a validated methodology for estimating the natural sloshing of the liquid, within the different vehicle chambers.

II. EXPERIMENTAL SETUP

The testing vehicle consisted of an articulated T2-S3 truck, with two axles in the tractor and three axles in the semitrailer [5]. Figure 3 illustrates this vehicle, which contained eight compartments or chambers, with different capacities, as it is listed in Table 1. The total capacity of the semitrailer tank was 41 000 liters, and was loaded at 66.5%, as an average. The instrumentation for the vehicle included speed, acceleration and pressure sensors. Chambers 1 and 5 were instrumented with pressure sensors, as it is shown in Figure 4. These sensors were installed at the mid height of the chamber walls, and had a full range capacity of 5 bar. Three accelerometers were mounted in the vehicle, with a range capacity of up to 50 g. The data acquisition system operated at a sample rate of 1 Hz. Global positioning system (GPS) devices were used to obtain the instantaneous speed of the vehicle.

The testing procedure consisted of sequences of braking maneuvers from different initial speeds. Each braking test was followed by a resting period of time.

The reasons for instrumenting chambers 1 and 5, derive from the different vertical and longitudinal dimensions that these chambers have with respect to each other. While chamber 1 is the largest of the chambers; it has the minimum vertical dimension. Consequently, the study could reveal the potential effects of these geometrical characteristics, on the pressure developed in each of the

chambers' wall.

The pressures developed in each of these chambers, has a direct connection with the level of stresses and consequently, with the reliability and fatigue life of these particular components. Figure 5 illustrates the instrumentation within a chamber while being filled with the working fluid (water).

III. SIMPLIFIED MODEL

The simplified model to simulate the sloshing cargo-vehicle interaction is based upon the integration of three different dynamic models, as follows: i) a multibody vehicle model, integrating the sprung and sprung masses of the



Fig. 3. Testing road tanker at BAM facilities.

TABLE I
 FILL CONDITIONS OF THE ROAD TANKER

Chamber	Nominal volume	Filling volume	% Fill
I	7500	4988	66.5
II	7500	4988	66.5
III	3000	1995	66.5
IV	3500	2328	66.5
V	5000	3325	66.5
VI	4000	2660	66.5
VII	3000	1995	66.5
VIII	7500	4988	66.5
Total	41000	27267	66.5

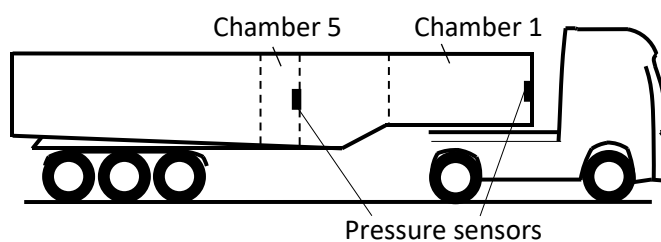


Fig. 4. Schematic representation of the vehicle and the location of the instrumented chambers.

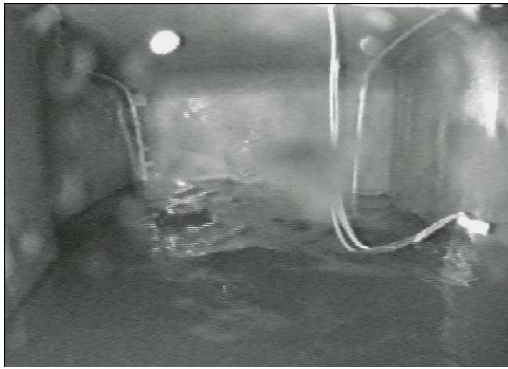


Fig. 5. The chamber No.5 in the process of being filled.

vehicle; ii) a sloshing cargo model represented by a simple pendulum whose characteristics are defined on the basis of a validated formulation; and iii) an on/off antilock brake system (ABS), which is set for the maximum braking coefficient of 0.75 for a wheel sleep of 0.2.

The equation of motion for the multibody system comprising the sprung and sprung masses of the vehicle, were obtained through the application of the Newton's law to the different masses of the vehicle. The resulting set of equations were manipulated in such a way that a first order system was obtained. The Transition Matrix Approach is thus used to simulate the response of such a system to the inputs deriving from the braking maneuver.

The resultant set of second order equations associated to the use of Newton's Second Law to each of the sprung and un-sprung masses, is expressed as matrix expressions of first order system, according to the following expression:

$$\left\{ \dot{y}(t) \right\} = [A]\{y(t)\} + [B]\{Y(t)\} \quad (3)$$

where the vector $\{y(t)\}$ contains the several degrees of freedom associated to the multibody vehicle, including, sequentially the function and its derivative; $[A]$ and $[B]$ are coefficient matrices, whose terms depend on the properties of the mechanical components included in the system, such as the mass, stiffness, damping and dimensions. $\{Y(t)\}$ in this equation represents the perturbation to the resulting mechanical system, containing the perturbation terms in relation with the different degrees of freedom of the mechanical system. According to the Transition Matrix approach, the discrete solution in the time domain of Eq. 3, results a recursive solution that depends on the previous state, as follows [6].:

$$\{y(t + dt)\} = [\Phi]\{y(t)\} + [\Gamma]\{Y(t)\} \quad (4)$$

where matrix $[\Phi]$ is the free response matrix of the system, which is called transition matrix, as it relates the present state $(t + \Delta t)$, with the previous state (t) . This matrix is calculated in general, through a Taylor expansion, according to the following equation:

$$[\Phi] = e^{[A]\Delta t} = [I] + [A]\Delta t + \frac{[A]^2 \Delta t^2}{2!} + \dots + \frac{[A]^n \Delta t^n}{n!} \quad (5)$$

The other matrix $[\Gamma]$ is the part of the solution that represents the particular response. This matrix is obtained by using the following expression, which represents a convolution integral:

$$[\Gamma] = \int_0^{\Delta t} e^{[A](\Delta t - t)} [B] dt = [A]^{-1} ([\Phi] - [I]) [B] \quad (6)$$

The sloshing of the fluid in the different chambers, is simulated through the pendulum analysis, according to which it is possible to simulate the first mode of vibration of the free surface of a liquid within a rectangular container, in terms of the oscillation angle of a simple pendulum whose length corresponds to the natural frequency of the liquid in the container. Figure 6 illustrates, schematically, the fundamental sloshing mode of the liquid inside chambers 1 and 5. According to this analogy, the pendulum representing the sloshing cargo is subjected to the longitudinal accelerations derived from the braking manoeuvre, and the oscillation angle will correspond to the angle of the liquid free surface.

The length of the pendulum in this analogy model, is obtained through calculating the natural sloshing frequency of the fluid inside the tank. For that, the principle of gravity waves is used, according to which, such frequency depends on the gravity acceleration; on the depth of the fluid; and on the length of the free surface. This model is valid for ideal fluids, and has been validated through experiments reported in the literature [7]. The formula is as follows:

$$c = \lambda f = \sqrt{\left(\frac{g}{\kappa} \tanh \kappa h \right)} \quad (7)$$

where c represents the velocity of the sloshing wave in the container (m); λ is the wavelength of the sloshing wave (m); f represents the natural sloshing frequency of the contained liquid (Hz); κ is called wave number, given by $\kappa = 2\pi / \lambda$; g is the local gravity acceleration (9.81 m/s^2); h is the depth of the liquid. In this equation, it is important to note that the wavelength λ is two times free surface length of the liquid (L). This gravity waves model is now used to characterize the sloshing characteristics of the fluid within the two instrumented chambers. For that, it is thus necessary to know the geometrical characteristics of the chambers along the direction of propagation of the waves, that in this case corresponds to the longitudinal axis of the different chambers/vehicle.

Figure 7 illustrates the dimensions taken as the base in the case of chambers 1 and 5, including the depth of the contained fluid in each of these chambers. As it can be observed in this figure, chamber 1 would have the lower frequency of vibration, due to the larger longitude.

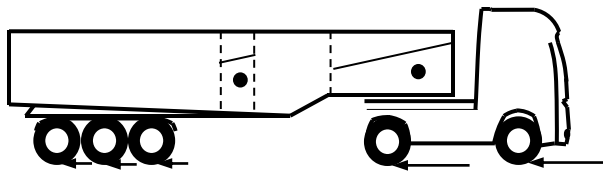


Fig. 6. First modes of vibration of the fluids in chambers 1 and 5.

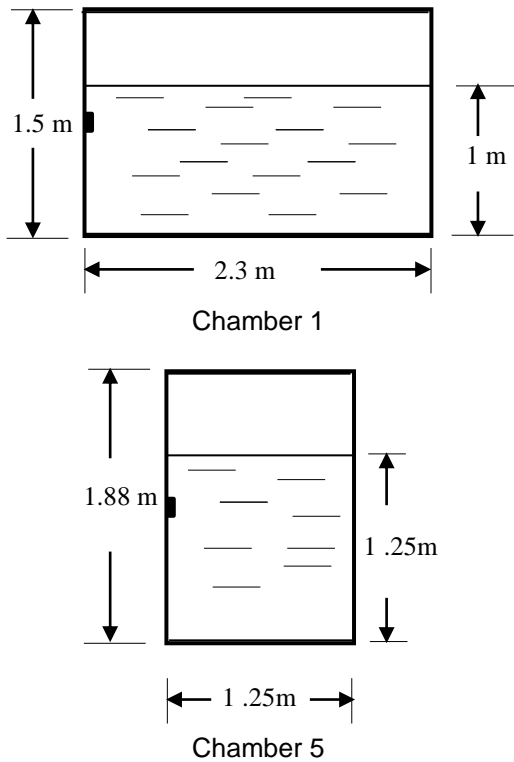


Fig. 7. Dimensions of the two instrumented chambers.

Using the gravity waves methodology expressed in Eq. (7) Figure 8 illustrates the resulting free sloshing frequencies for the fluid in chamber 1 and 5. As expected, the lower natural frequency is obtained in the case of the chamber No. 1. The length of the respective simple pendulums l_p , is obtained according to the basic formula for a simple pendulum:

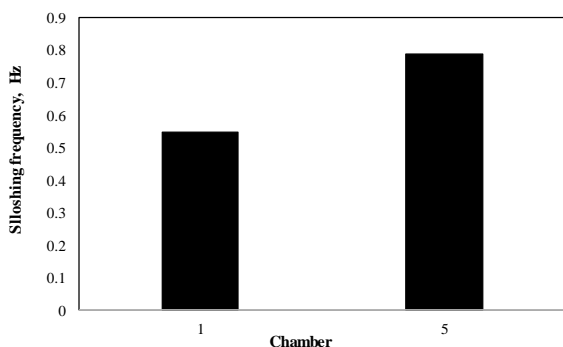


Fig. 8. Natural frequencies of the liquid inside the instrumented chambers.

$$f_p = \frac{1}{2\pi} \sqrt{\frac{g}{l_p}} \quad (8)$$

where g is the acceleration due to gravity. The resulting lengths are as follows:

- Chamber 1 : 0.833 m
- Chamber 5 : 0.393 m

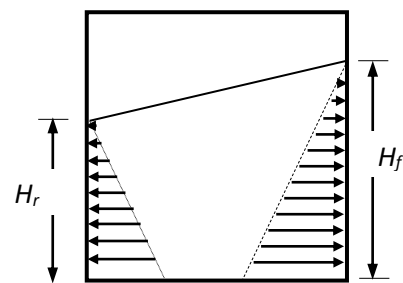
The pressure on the walls of each chamber is obtained by calculating the superposition of a longitudinal pressure and a vertical pressure. While the longitudinal pressure is a function of the acceleration and on the length of the horizontal length of fluid, the vertical pressure is calculated through the consideration of the instantaneous height of the fluid on the wall. This is illustrated in Figure 9. Consequently, the pressure on the larger chamber would be greater than in the shorter chamber. For example, the hydrostatic at the bottom of the chamber illustrated in Figure 9, due to the gravity (p_v) is given by:

$$p_v = \gamma H_f; \quad (9)$$

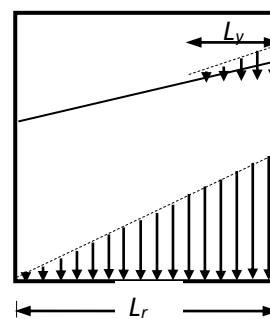
where γ is the specific weight of the fluid. On the other hand, the longitudinal pressure (p_L) is expressed by the following equation, in terms of the longitudinal acceleration a_L :

$$p_L = \rho a_L L_r; \quad (10)$$

where ρ is the mass density of the fluid.



Hydrostatic pressure due to fluid's weight



Hydrostatic pressure due to fluid's acceleration

Fig. 9. Hydrostatic pressures on the compartment walls.

IV. RESULTS

Figure 10 illustrates the theoretical results from the simplified model considered, together with the experimental data. These results and measurements are presented one next to the other, in order to facilitate the validity analysis of the proposed simulation methodology.

These results illustrate that the trends are comparable for both sets of data, that is, a similar range is obtained for all of the variables reported. A lower pressure is generated in chamber 5, which is attributed to the shorter length of this chamber. However, such increase in pressure does not correspond exactly to the difference of lengths, as the ratio of lengths would cause a differential pressure of $2.3/1.23 = 1.86$, while the ratio of average pressures is on the order of 2. That is, there is an incremental, which is associated to the maximum height attained by the fluid in the chamber.

The major difference between both sets of data, the experimental and theoretical, is that the theoretical do not include much of the noise and random oscillations reported in the experimental data. Such noise, however, is of very low amplitude, in comparison with the maximum values attained.

The practical applications of these results could be in the area of chamber design, so that the effects of the length of the chambers be taken into account. That is, such greater lengths for the fluid in the chamber would involve larger pressures and consequently, greater stresses. However, the analysis should include an overall perspective, that is, the shortening of the chambers would imply an increase in the number of chambers, for a certain total payload, and the superposition effect of pressures, should be considered.

On the other hand, the analysis could be extended to characterize the effects of the distribution of the lengths of the different chambers along the axis of the tanker, as the different resulting forces could have different effects on the pitch response of the road tanker.

V. CONCLUSION

A simplified model, based upon physical principles, is proposed to simulate the effect of sloshing on the pressure developed in the tanker chambers. The model has been validated in good extent, with experimental data from full scale testing. The characteristic that mostly affects the pressure developed with the chambers of the tanker is the length of the chamber. While a reduction in this property could decrease the pressure developed within a given chamber, the analysis should take into account an overall approach, as a shortening of the individual chambers would influence the number of chambers necessary to carry a certain amount of product. Consequently, the resulting model could be used to study different effects of the sloshing cargo on the carrying vehicles, including the length and position of the chambers along the tanker body.

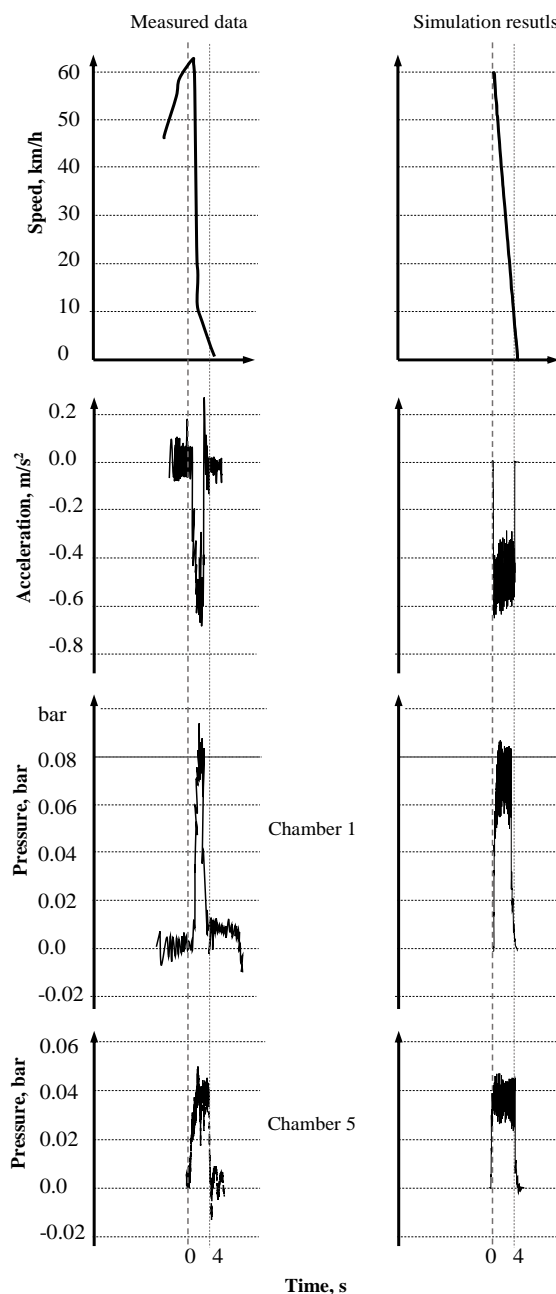


Fig. 10. Simulation and measured data.

REFERENCES

- [1] Raouf A., I., *Handbook of Structural Life Assessment*, Wiley, 2017.
- [2] Yang, F., Yan, G., Rakheja, S., "Anti-slosh Effectiveness of Baffles and Braking Performance of a Partly-Filled Tank Truck", *Applied Mechanics and Materials*, 2014. 541-542: 674-683.
- [3] Romero, J. A., Lozano-Guzmán, A.A., Obregón-Biosca, S.A., Betanzo-Quezada, E. "A heavy truck - infrastructure interaction model", *Proceedings of the Fifteen International Conference on Civil, Structural and Environmental Engineering Computing*, 2015. p. 213.
- [4] Romero, José A., Lozano, A.A., Betanzo-Quezada, E., and Arroyo-Contreras, G.M., "Cargo securement methods and vehicle braking performance", *International Journal of Vehicle Performance* 2(4): 353-373.
- [5] BAM, 2004, *Sloshing tests on a tanker semi-trailer*, Federal Institute for Materials Research and Testing (BAM), Hazardous goods tanks and accident mechanics, 2004. (In German)
- [6] Meirovitch, L., *Elements of vibration analysis*, Mc Graw Hill Int., 2nd ed., 1986.
- [7] Cushman-Roisin, B. *Environmental fluid mechanics*, John Wiley & Sons, Inc., 2014, N.Y.